Chemical Science

ROYAL SOCIETY OF CHEMISTRY

EDGE ARTICLE

View Article Online
View Journal | View Issue

Cite this: *Chem. Sci.*, 2022, **13**, 3999

All publication charges for this article have been paid for by the Royal Society of Chemistry

Hydridotetrylene [Ar*EH] (E = Ge, Sn, Pb) coordination at tantalum, tungsten, and zirconium†

Max Widemann,[a] Sebastian Jeggle,[a] Maximilian Auer,[a] Klaus Eichele,[a] Hartmut Schubert,[a] Christian P. Sindlinger *[b] and Lars Wesemann *[a]

In a reaction of tantalocene trihydride with the low valent aryl tin cation $[Ar^*Sn(C_6H_6)][Al(OC\{CF_3\}_3)_4]$ (**1a**) the hydridostannylene complex $[Cp_2TaH_2{-}Sn(H)Ar^*][Al(OC\{CF_3\}_3)_4]$ (**2**) was synthesized. Hydride bridged adducts $[Cp_2WH_2EAr^*][Al(OC\{CF_3\}_3)_4]$ (E = Sn **3a**, Pb **3b**) were isolated as products of the reaction between Cp_2WH_2 and cations $[Ar^*E(C_6H_6)][Al(OC\{CF_3\}_3)_4]$ (E = Sn **1a**, Pb **1b**). The tin adduct **3a** exhibits a proton migration to give the hydridostannylene complex $[Cp_2W(H){=}Sn(H)Ar^*][Al(OC\{CF_3\}_3)_4]$ **4a**. The cationic complex **4a** is deprotonated at the tin atom in reaction with base ^{Me}NHC at 80 °C to give a hydrido-tungstenostannylene $[Cp_2W(H)SnAr^*]$ **5a**. Reprotonation of metallostannylene **5a** with acid $[H(Et_2O)_2][BAr^F]$ provides an alternative route to hydridotetrylene coordination. Complex **4a** adds hydride to give the dihydrostannyl complex $[Cp_2W(H){-}SnH_2Ar^*]$ (**7**). With styrene **4a** shows formation of a hydrostannylation product $[Cp_2W(H){=}Sn(CH_2CH_2Ph)Ar^*][Al(OC\{CF_3\}_3)_4]$ (**8**). The lead adduct **3b** was deprotonated with ^{Me}NHC to give plumbylene **5b** $[Cp_2W(H)PbAr^*]$. Protonation of **5b** with $[H(Et_2O)_2][Al(OC\{CF_3\}_3)_4]$ at −40 °C followed by low temperature NMR spectroscopy indicates a hydridoplumbylene intermediate $[Cp_2W(H){=}Pb(H)Ar^*]^+$ (**4b**). Hydrido-tungstenotetrylenes of elements Ge (**5c**), Sn (**5a**) and Pb (**5b**) were also synthesized reacting the salt $[Cp_2W(H)Li]_4$ with organotetrylene halides. The metallogermylene $[Cp_2W(H)GeAr^*]$ (**5c**) shows an isomerization *via* 1,2-H-migration to give the hydridogermylene $[Cp_2W{=}Ge(H)Ar^*]$ (**9**), which is accelerated by addition of AIBN. **9** is at rt photochemically transferred back to **5c** under light of a mercury vapor lamp. Zirconocene dihydride $[Cp_2ZrH_2]_2$ reacts with tin cation **1a** to give the trinuclear hydridostannylene adduct **10** $[(\{Cp_2Zr\}_2\{\mu\text{-}H\})(\mu\text{-}H)_2\mu\text{-}Sn(H)Ar^*][Al(OC\{CF_3\}_3)_4]$. Deprotonation of **10** was carried out using benzyl potassium to give neutral $[(\{Cp_2Zr\}_2\{\mu\text{-}H\})(\mu\text{-}H)\mu\text{-}Sn(H)Ar^*]$ (**11**). **11** was also obtained from the reaction of low valent tin hydride $[Ar^*SnH]_2$ with two equivalents of $[Cp_2ZrH_2]_2$. The trihydride Ar^*SnH_3 reacts with half of an equivalent of $[Cp_2ZrH_2]_2$ under evolution of hydrogen and formation of a dihydrostannyl complex **13** $[Cp_2Zr(\mu\text{-}H)SnH_2Ar^*]_2$ and with further equivalents of Ar^*SnH_3 to give bis(hydridostannylene) complex $[Cp_2Zr\{Sn(H)Ar^*\}_2]$.

Received 17th January 2022
Accepted 21st February 2022

DOI: 10.1039/d2sc00297c

rsc.li/chemical-science

Introduction

The coordination chemistry of tetrylenes [ER_2; E = Si, Ge, Sn, Pb; R = aryl, alkyl, amide, alkoxide, silyl] has been studied successfully over the last fifty years.[1–12] While numerous examples of tetrylene transition metal complexes and reports on their chemistry have been published, there is only a small number of hydridotetrylene coordination compounds in the literature. Hydridotetrylene complexes were synthesized by chloride abstraction from chlorosilyl or germyl ligands and by chloride abstraction from transition metal substituted chloride complexes followed by a 1,2-H migration (Scheme 1).[13–15] The research groups of Tilley and Tobita developed the alkane elimination route for the syntheses of hydridotetrylene coordination compounds by reacting organometallic alkyl complexes with organoelement trihydrides of Si, Ge, and Sn (Scheme 1). After transfer of the tetryl group to the transition metal, an open coordination site allows 1,2-H migration to give the hydridotetrylene ligand.[16–28] Recently Power *et al.* presented an example for a nucleophilic substitution using the low valent tin hydride Ar*SnH [Ar* = 2,6-$Trip_2C_6H_3$, Trip = 2,4,6-triisopropylphenyl] as a ligand to replace a coordinating THF (Scheme 1).[29] This research group investigated the coordination chemistry of anions $[Ar^*GeH_2]^-$ and $[Ar^*SnH_2]^-$ in reaction with group 4 metallocene dihalides. Interestingly after substitution of the halides, the stannyl complexes spontaneously eliminate

[a]*Institut für Anorganische Chemie, Auf der Morgenstelle 18, 72076 Tübingen, Germany. E-mail: lars.wesemann@uni-tuebingen.de*

[b]*Institut für Anorganische Chemie, RWTH Aachen University, Landoltweg 1a, D-52074 Aachen, Germany. E-mail: christian.sindlinger@ac.rwth-aachen.de*

† Electronic supplementary information (ESI) available: Full characterization, NMR spectra, DFT details and XYZ coordinates. CCDC 2142080–2142089. For ESI and crystallographic data in CIF or other electronic format see DOI: 10.1039/d2sc00297c

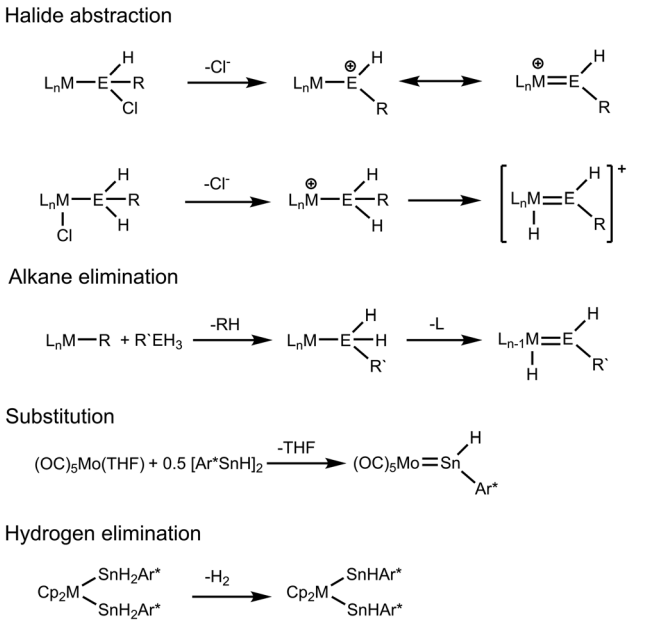

Scheme 1 Reported synthetic methods for hydridotetrylene complexes.

hydrogen to give the bis(hydridostannylene) coordination compounds (M = Zr, Hf).[30] Stabilized as N-heterocyclic carbene adducts, dihydrogermylene and stannylene were synthesized and coordinated as ligands at tungsten pentacarbonyl fragments.[31,32]

Low-coordinate cations of heavy Group 14 elements are attractive compounds for reactivity studies.[33] Due to their high sensitivity, preparation of these cations was realized using bulky ligands.[34,35] Cp* ligands as well as terphenyl derivatives are prominent substituents in this context and cations like $[Cp^*E]^+$ (E = Ge, Sn, Pb) and $[Ar^*E\text{–}L]^+$ (E = Sn, L = NHC, P*t*Bu$_3$; E = Pb, L = toluene) were reported.[34,36–40] Furthermore, amides provided with sterically demanding groups stabilize Group 14 element cations, which exhibit further contacts with flanking aryl or imine groups.[41–43] Chelating ligands like diketiminates or aminotroponiminates have also been employed for synthesis of low-coordinate cations of Ge, Sn and Pb.[44,45] So far, reactivity studies of those low valent cations focus on studies of oxidative additions.[33,35,46] Thus, Tobita and co-workers studied insertion of a cationic metallogermylene into E–H bonds (E = H, B, and Si).[35] We present in this publication reactions of low-valent Group 14 cations of Sn and Pb with bis(cyclopentadienyl) hydrides of zirconium, tantalum and tungsten resulting in the formation hydridotetrylene coordination compounds. The metallocene hydrides were chosen because of their good accessibility and different electron configurations. In the case of germanium, a reversible interconversion between a coordinated hydridogermylene and hydrido-metallogermylene is presented.

Results and discussion

Both starting materials, the low valent cations of tin and lead, were synthesized straightforwardly as salts of weakly coordinating anions. Low valent hydrides of tin and lead $[(Ar^*EH)_2]$ (E = Sn, Pb)[47–49] stabilized by a bulky terphenyl substituent Ar* [Ar* = 2,6-Trip$_2$C$_6$H$_3$, Trip = 2,4,6-triisopropylphenyl] were reacted with the hydride abstraction reagent $[Ph_3C][Al(OC\{CF_3\}_3)_4]$ to give yellow $[Ar^*Sn\text{–}L][Al(OC\{CF_3\}_3)_4]$ (**1a**) and orange $[Ar^*Pb\text{–}L][Al(OC\{CF_3\}_3)_4]$ (**1b**) as crystalline material (L = solvent benzene).[37,39,47–51]

Dissolved in 1,2-difluorobenzene (*o*-DFB) the cations were reacted with one equivalent of a benzene solution of tantalocene trihydride Cp$_2$TaH$_3$. In the case of the tin cation a product was selectively formed (Scheme 2) and in the lead case a mixture of undefined reaction products was obtained. The tantalum complex **2** was isolated by crystallization and in Fig. 1 the molecular structure of the cation of **2** is depicted.

In the cationic tantalum complex **2** a Ta–Sn bond is formed, and a hydride is transferred from the tantalum atom to the tin atom resulting in coordination of hydridoorgano stannylene [Ar*SnH]. The Ta–Sn bond length of 2.7207(2) Å can be compared with the Ta–Sn bond [2.752(1) Å] found in complex Cp$_2$TaH$_2$(SnCl$_2$CH$_3$).[52] The LUMO of cation **2** shown in Fig. 1 exhibits to a larger extent an empty p-orbital at the tin atom. In the ^{1}H NMR for the Ta–H units a doublet was found at −3.75 ppm ($^3J_{HH}$ = 1.4 Hz), also showing coupling with the tin atom ($^2J_{SnH}$ = 300 Hz). The signal for the Sn–H unit (t, $^3J_{HH}$ = 1.7 Hz) was found at a relatively high frequency, 15.55 ppm,

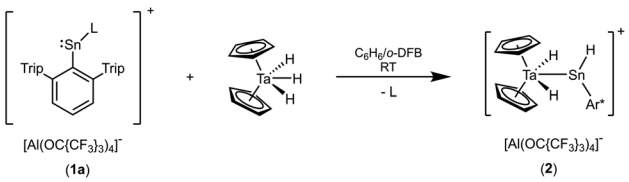

Scheme 2 Reaction of the low valent tin cation of **1a** with Cp$_2$TaH$_3$ (L = C$_6$H$_6$).

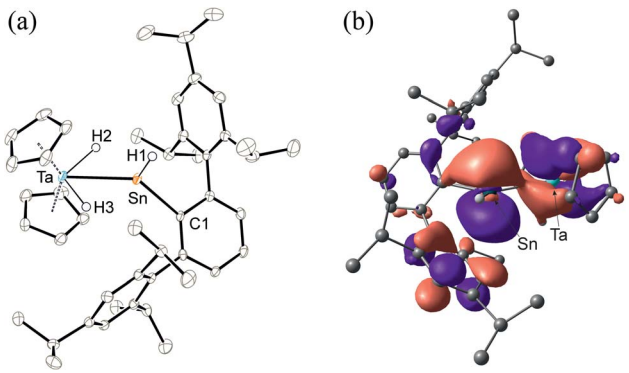

Fig. 1 Left: ORTEP of the molecular structure of the cation of **2**. Thermal ellipsoids are shown at 50% probability level. The anion [Al(OC{CF$_3$}$_3$)$_4$]$^-$ as well as co-crystallised 1,2-difluorobenzene have been omitted. Selected interatomic distances [Å] and angles [°]: Ta–Sn 2.7207(2), Sn–C1 2.161(3), Ta–H3 1.770(19), Ta–H2 1.81(3), Sn–H1 1.68(4), Sn–H2 2.18(3), Ta–Cp 2.372(3)–2.402(3), Ta–Sn–H1 115.7(14), Ta–Sn–C1 133.3(1); right (mirrored perspective): LUMO of the cation of **2**.

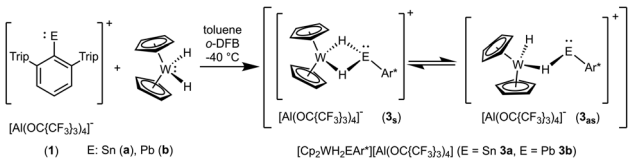

Scheme 3 Reaction of Cp_2WH_2 with low valent tin **1a** and lead **1b** cations.

showing a large $^1J_{Sn-H}$ coupling constant ($^1J_{SnH}$ = *ca.* 1040 Hz). Hydridostannylene coordination at osmium exhibits a comparable signal in the ^{1}H NMR spectrum [Cp*(^{i}Pr$_3$P)(H)Os=Sn(H) trip, ^{1}H NMR 19.4 ppm (SnH), $^1J_{SnH}$ = 775 Hz, ^{119}Sn NMR 786 ppm].[19] The ^{119}Sn NMR signal of **2** at 1161 ppm (dt, $^1J_{SnH}$ = 1047 Hz, $^2J_{SnH}$ = 308 Hz) can be compared with signals found for triply coordinate stannylium cations $[R_3Sn]^+$ (R = Trip 714 ppm, R = Dur 720 ppm, R = tBu$_2$MeSi 2653 ppm) (Trip = 2,4,6-iPr$_3$C$_6$H$_2$, Dur = 2,3,5,6-Me$_4$C$_6$H).[53–57] To rationalize the ^{119}Sn NMR data of **2**, NMR chemical shift calculations have been carried out using ORCA and ADF program packages.[58–60] The calculated chemical shift of the tin atom of **2** amounts to 981 ppm (exp. 1161 ppm). Furthermore, in the optimized structure of **2**, contacts between one of the aryl moieties of the terphenyl substituent and the tin atom were found. Thus, complex **2** can be regarded as a hydridostannylene complex with a stannylene acting as σ-donor ligand exhibiting no π-acceptor character. This results in an empty p-orbital at the tin atom and the triply coordinate tin atom can be regarded as a stannylium cation. Furthermore, a ^{119}Sn NMR signal at 1161 ppm lies in the range of known triply coordinate stannylium cations (*vide supra*) and therefore interactions of the TaH units with the stannylium cation of **2** can be excluded.

In contrast to tantalocene trihydride Cp_2TaH_3 the transition metal in tungstenocene dihydride Cp_2WH_2 is not in the maximum possible oxidation state but in state four and has two valence electrons. Reacting the cations $[Ar^*Sn]^+$ **1a** and $[Ar^*Pb]^+$ **1b** (see ESI for synthetic details†) with Cp_2WH_2 at low temperature (−40 °C) resulted in highly coloured reaction mixtures [E: Sn (**3a**) pink; Pb (**3b**) violet] (Scheme 3). Unlike complex **2**, the resulting products **3a** and **3b** do not show any hydride transfer to the main group metal, instead, coordination of the Cp_2WH_2 fragment *via* the hydride substituents at the electrophilic Group 14 element was found.

In the ^{1}H NMR spectrum both complexes **3a** and **3b** exhibit at rt a broad resonance for the hydride substituents [−10.83 (**3a**), −7.55 ppm (**3b**)]. Below −20 °C two different isomers are observable, a symmetric one (**3**$_s$): **3a**$_s$ −10.86 ppm, J_{W-H} 78 Hz; **3b**$_s$ −7.49 ppm, J_{W-H} 75 Hz; and an asymmetric one (**3**$_{as}$): **3a**$_{as}$ −11.13 ppm, J_{W-H} 51 Hz, −8.57 ppm, J_{W-H} 77 Hz; **3b**$_{as}$ −12.31 ppm, J_{W-H} 52 Hz, −4.30 ppm, J_{W-H} 76 Hz (signal at higher frequency corresponds to the bridging W–H–E unit). Only in the ^{1}H NMR spectra of **3a** ^{183}W satellites were unambiguously observed. Due to shorter relaxation times of the ^{119}Sn nucleus, tin satellites are expected to be broadened beyond recognition, however $^1J_{119Sn-H}$ coupling was observed in the ^{119}Sn NMR spectrum. These isomers have also been

Table 1 Characteristic data of the presented tantalum and tungsten complexes **2–9**

Compound (E)	^{1}H NMR M–H [ppm]	J^{183}_{W-H} [Hz]	^{1}H NMR E–H [ppm]	J_{E-H} (E: ^{119}Sn/^{207}Pb) [Hz]	^{119}Sn/^{207}Pb NMR [ppm]	^{183}W NMR	d M–E [Å]
2 (Sn)	−3.75		15.55	1040	1161		2.7207(2)
3a (Sn)							
3a$_s$	−10.86	78		*ca.* 270	1786	−3910	
3a$_{as}$	−11.13, −8.57	51, 77			1735	−4309	
3b (Pb)							
3b$_s$	−7.49	75			7986	−3994	
3b$_{as}$	−12.31, −4.30	52, 76				−4259	
4a (Sn)	−12.57	67	15.13	1193 (^1J), 129 (^2J)	1057	−3629	2.6221(2)
4b[a] (Pb)	−13.67	66	42.13	ca. 530			
4c (Ge)	−11.08	69	11.30			−3585	
5a (Sn)	−12.37	90			2883	−4182	2.7589(4)/2.7488(4)
5b (Pb)	−16.15	91			10 534	−2772	2.8226(2)
5c (Ge)	−11.03	92				−4079	
6 (Sn)	−13.82	63	6.33	1344 (^1J), 165 (^2J)	−231	−4378	
7	−12.91	66	5.12	1274, 1216	−236	−3921	2.7582(2)
8	−12.51	68		132 (^2J)	1223	−3526	
9			10.04			−3096	

[a] Not isolated, observed in solution as intermediate.

characterized by an ^{1}H–^{183}W-HMQC-NMR experiment at −40 °C featuring cross peaks for the symmetric and asymmetric isomer (see ESI for spectra†). Rocchigian, Bochmann and Hrobárik *et al.* reported recently on the different coordination modes of Cp_2WH_2 at Au(I)/Au(III) cations.[61] In the case of asymmetric hydride coordination a comparable ^{1}H NMR spectrum was observed: −11.4 ppm, J_{W-H} 48 Hz, −9.6 ppm, J_{W-H} 61 Hz.[61] Furthermore, chemical exchange of all hydrides in cations **3** was proven by ^{1}H–^{1}H EXSY NMR studies. For the characterization of the isomers by ^{119}Sn, ^{207}Pb and ^{183}W NMR spectroscopy see Table 1 and the ESI.† The chemical shift of the heteroatoms tin and lead in the hydride bridged complexes **3a** (^{119}Sn: 1786, 1735 ppm) and **3b** (^{207}Pb: 7986 ppm, ^{207}Pb NMR signal of other isomer was not observed) can be compared with the values found for the rhodium complexes showing a comparable structural motif [$(Ph_3P)_2RhH_2EAr^*$] [E = Sn 1728 ppm, E = Pb 8195 ppm].[62] The ^{183}W chemical shifts of **3a** and **3b** (Table 1) lie in the range known for metallocene hydride complexes of tungsten.[63–65] The ^{183}W chemical shift is more affected by the isomerism, symmetric or asymmetric (**3a**$_s$ *vs.* **3a**$_{as}$, **3b**$_s$ *vs.* **3b**$_{as}$: ≈300–400 ppm), than the nature of the tetrel, tin or lead (**3a**$_s$ *vs.* **3b**$_s$, **3a**$_{as}$ *vs.* **3b**$_{as}$: ≈35–80 ppm).

Using a slight excess of Cp_2WH_2 in the synthesis of **3a** (E: Sn), the deep pink solution decolourises to orange to form the cationic hydridotungsten hydridostannylene complex **4a**. Presumably, mediated by the basic Cp_2WH_2, as a proton-shuttle, a tungsten-bound proton of **3a** migrates to Sn and a W–Sn bond is formed.[66] The model of a proton-migration mediated by a Bronsted-basic Cp_2WH_2 is corroborated by the observation that addition of amine-bases such as diethyl methylamine to isolated **3a** equally enables the isomerization (Scheme 4). The molecular structure of the cation of **4a** is shown in Fig. 2. The W–Sn bond length of 2.6221(2) Å is shorter than typical single bonds (2.68–2.81 Å)[2,67–71] between these elements and longer than the W–Sn triple bond (2.46–2.50 Å).[72,73] In quantum chemical calculations π-donation from tungsten to the empty p-orbital at tin atom was found in addition to a W–Sn σ-bond (see ESI† for details of DFT calculations using ORCA and NBO analysis).[58,59,74] The short W–Sn bond in **4a** together with the slight π-donation from W to the empty p-orbital at tin might be interpreted as an indicator for partial double bond character between tin and tungsten. In the ^{1}H NMR spectrum the signals of the hydride units in **4a** (W–H −12.73 ppm, Sn–H 15.13 ppm) were found at frequencies typical for Cp_2WH-fragments and hydridostannylene coordination.[19,22,30,61] The $^{1}J_{Sn-H}$ coupling constant of 1193 Hz lies close to the values found in **2** and in the literature examples $[Cp_2M(Ar^*SnH)_2]$ M: Ti 1250 Hz, Zr 1125 Hz, Hf 1060 Hz.[30] In the ^{119}Sn NMR spectrum the signal was found at 1057 ppm corroborating stannylene coordination at transition metals.[19,75] Deprotonation of **4a** was carried out in reaction with a N-heterocyclic carbene 1,3,4,5-tetramethylimidazol-2-ylidene (^{Me}NHC) at 80 °C in toluene/1,2-

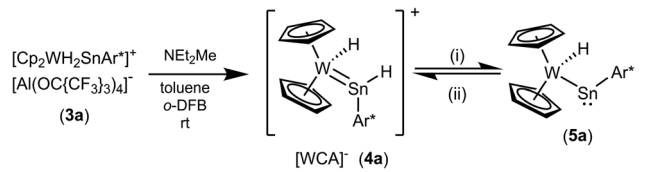

Scheme 4 (i) ^{Me}NHC, toluene/$C_6H_4F_2$, 70 °C, 3 d, – [^{Me}NHC–H][Al(OC{CF_3}$_3$)$_4$], (ii) [$H(Et_2O)_2$][BAr^F] toluene/*o*-DFB. {[B(3,5-{CF_3}$_2C_6H_3$)$_4$]$^-$ = [BAr^F]$^-$}.

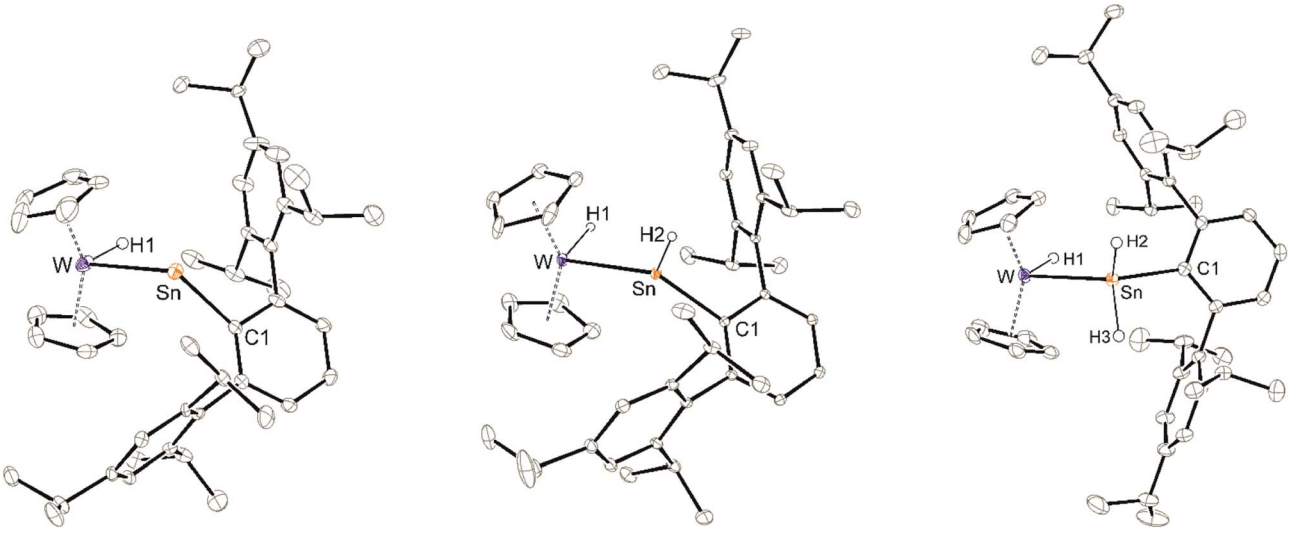

Fig. 2 ORTEP of the molecular structures of **5a**, **4a** and **7**. Thermal ellipsoids are shown at 50% probability level. Hydrogen atoms except the W–H and Sn–H units and the anion of **4a** have been omitted. Selected interatomic distances [Å] and angles [°]: **5a**, W–Sn 2.7589(4), W–Cp 2.266(5)–2.330(5), Sn–C1 2.264(4), W–Sn–C1 108.3(1); **4a**,W–Sn 2.6221(2), Sn–H2 1.60(5), W–Cp 2.282(4)–2.330(4), Sn–C1 2.144(2), W–Sn–C1 138.64(6), H1–W–Sn 90.0(18), W–Sn–H2 119.5(18), H2–Sn–C1 101.8(18); **7**, W–Sn 2.7582(2), Sn–C1 2.196(3), W–Cp 2.247(3)–2.357(3), W–H1 1.69(5), Sn–H2 1.76(3), Sn–H3 1.76(3), W–Sn–C1 134.1(1), H1–W–Sn 87.0(15), W–Sn–H2 108.5(14), W–Sn–H3 112.8(10), H2–Sn–C1 100.1(14), H3–Sn–C1 97.6(10).

difluorobenzene (Scheme 4). The colour of the solution changes from orange to yellow to green and metallostannylene **5a** was isolated after crystallization in a yield of 44%. The molecular structure of **5a** is presented in Fig. 2. The W–Sn bond length of 2.7589(4) Å is a short single bond for a metallostannylene of tungsten (*vide supra*).[76,77] Comparing the W–Sn bond lengths in **4a** [2.6221(2) Å] and **5a** [2.7488(4) Å], due to the partial double bond character, found for **4a**, the protonated derivative **4a** exhibits a shorter W–Sn length. In the ^{119}Sn{^{1}H} NMR spectrum of **5a** a signal at high frequency of 2883 ppm indicates a metallostannylene.[76] The signal for the W–H hydride of **5a** was found in the ^{1}H NMR spectrum in the typical range for transition metal hydrides at −12.37 ppm. Reprotonation of metallostannylene **5a** at the tin atom was achieved in reaction with the acid $[H(Et_2O)_2][BAr^F]$[78] to give the cationic hydridostannylene complex **4a**, now with the weakly coordinating anion $[BAr^F]^-$ (Scheme 4). Thus, protonation of metallostannylene complexes is an alternative route for the synthesis of hydridotetrylene coordination compounds.

Deprotonation of the cation **4a** was achieved with ^{Me}NHC at 80 °C (Scheme 4). Reacting the cation with the carbene at rt an adduct (Scheme 5, **6**) of the N-heterocyclic carbene at the tin was isolated and characterized by NMR spectroscopy. This adduct **6** is also the product of the reaction between **3a** and ^{Me}NHC. Heating this adduct **6** to 80 °C gives the deprotonation product **5a**. Tobita *et al.* studied the NHC-induced conversion of hydrido(hydrogermylene) complexes into a germylyne coordination compound. In this stepwise procedure NHC-adduct formation was found followed by deprotonation of a W–H unit by the NHC.[79,80] The reactivity of the cationic arylhydridostannylene complex **4a** was investigated in reaction with $LiAlH_4$ (Scheme 6) and styrene (Scheme 7). Nucleophilic attack of a hydride anion at the tin atom of cation **4a** was observed in reaction with $LiAlH_4$. The aryldihydridostannyl ligand coordinates at the tungsten atom in complex **7** with a W–Sn bond length of 2.7582(2) Å.[2,67–71] The reverse reaction, hydride abstraction from complex **7** was also investigated in reaction with the trityl salt $[Ph_3C][Al(OC\{CF_3\}_3)_4]$ to give the salt **4a** in moderate yield of 71% based on results of NMR spectroscopy (Scheme 6). Direct addition or elimination of hydrogen (to transfer of **5a** into **7** or **7** into **5a**) was not observed (heating or photochemical activation of **7**, addition of hydrogen to **5a**, 1–3.5 atm). However, stepwise addition and abstraction of protons and hydride ligands is a possible pathway for the reversible conversion of **5a** into **7** (Scheme 4 and 6).

With an excess of styrene, hydride complex **4a** exhibits hydrostannylation of the olefin at 75 °C (Scheme 7). Insertion of olefines and carbon dioxide into the Sn–H bond of low valent organotinhydrides was studied by Power *et al.* and for a coordinated organohydrido germylene another example of styrene insertion is presented in the literature.[14,29,81]

In the case of the low valent lead cation the tungstenocene dihydride adduct **3b** does not exhibit a hydrogen atom migration from tungsten to lead as in the case of the tin compound **3a**. Lead adduct **3b** was readily deprotonated at rt by ^{Me}NHC to yield the plumbylene complex **5b** (Scheme 8). Evidence for the formation of an NHC adduct comparable to **6** was not found. Plumbylene **5b** was crystallized from a pentane solution at −40 °C (see Fig. 3 for ORTEP of the molecular structure). The W–Pb distance of 2.8226(2) Å found in **5b** is shorter than the W–Pb distance in the plumbylene $[Cp(CO)_3W–PbAr^*$, W–Pb 3.006(1) Å].[82] Furthermore the ^{207}Pb NMR resonance of **5b** was observed at a very high frequency of 10 534 ppm $[Cp(CO)_3W–PbAr^*$ ^{207}Pb NMR 9374 ppm].[82] Protonation of **5b** was carried out at −40 °C using $[H(Et_2O)_2][Al(OC\{CF_3\}_3)_4]$ as the proton source (Scheme 8). The cold reaction mixture was directly investigated by low temperature ^{1}H NMR spectroscopy. Besides signals of the starting material **5b**, and the product **3b** two new signals at very low (−13.67 ppm) and very high (42.13 ppm) frequencies were detected. Based on a ^{1}H–^{1}H–COSY-LR-NMR experiment (see ESI†) both signals belong to the same compound. Furthermore, the signal at high frequency exhibits both ^{207}Pb- (530 Hz) and ^{183}W-satellites (39 Hz). In the case of the low frequency signal ^{183}W-satellites (66 Hz) were observed.

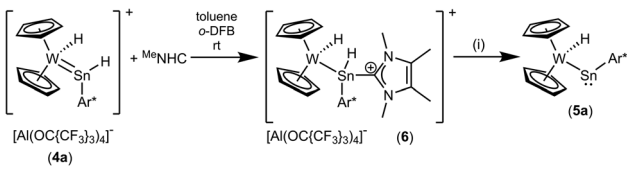

Scheme 5 (i): Toluene/*o*-DFB, 80 °C, 3d, – $[^{Me}NHC–H][Al(OC\{CF_3\}_3)_4]$.

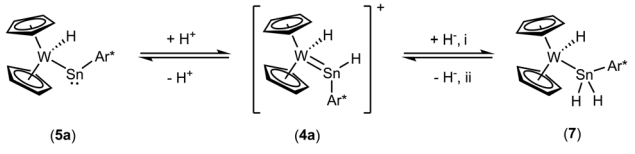

Scheme 6 Addition and abstraction of protons and hydride ligands. (i): rt, $LiAlH_4$, Et_2O; (ii): rt, $[Ph_3C][Al(OC\{CF_3\}_3)_4]$, *o*-DFB.

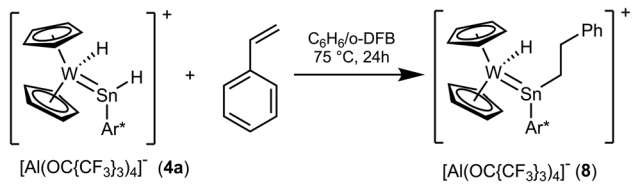

Scheme 7 Insertion of styrene into a Sn–H bond.

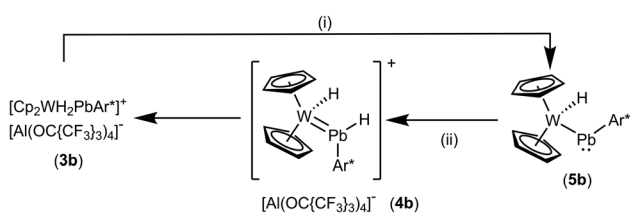

Scheme 8 (i): + ^{Me}NHC, toluene/*o*-DFB, rt, 3 h, – $[^{Me}NHC–H][Al(OC\{CF_3\}_3)_4]$, (ii): + $[H(Et_2O)_2][Al(OC\{CF_3\}_3)_4]$, toluene/$C_6H_4F_2$, rt, – 2 Et_2O.

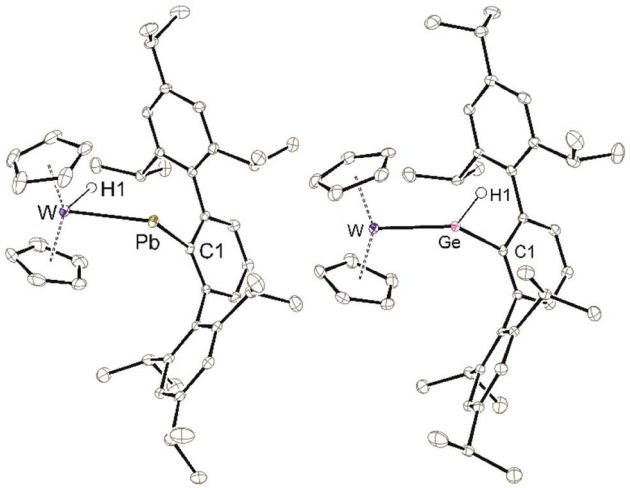

Fig. 3 ORTEP of the molecular structures of **5b** and **9**. Thermal ellipsoids are shown at 50% probability level. Hydrogen atoms except the W–H and Ge–H units have been omitted. Selected interatomic distances [Å] and angles [°]: **5b**, W–Pb 2.8226(2), W–Cp 2.260(3)–2.330(3), Pb–C1 2.353(3), W–Pb–C1 110.1(1); **9**, W–Ge 2.4271(3), W–Cp 2.248(2)–2.310(2), Ge–C1 1.984(2), Ge–H 1.53(2), W–Ge–C1 134.7(1).

Due to comparable spectroscopic data, we speculate about the structure of this intermediate **4b** and suggest a hydridoplumbylene motive like in the tin case **4a**. Based on this molecular structure of **4a** the tin atom was exchanged against a lead atom and this structure was optimized using DFT calculations (see ESI for details†).[58,59] This optimized structure was used for chemical shift calculations of the protons with the ADF program package.[60] The results of these calculations [PbH exp. 42.13 ppm, calc. 39.3 ppm and WH exp. −13.67 ppm, calc. −11.5 ppm] lie close to the experimentally observed signals. This extreme high frequency chemical shift of the PbH unit at 42.13 ppm can be explained with the spin–orbit coupling of the heavy atom with the light atom (SO-HALA effect).[83] This effect was already observed for low valent lead hydride exhibiting a ^{1}H NMR signal at 35.61 ppm.[49] However, **4b** is only an intermediate in the protonation of **5b** and the isolation was not possible, which could be due to the weak Pb–H bond. With these NMR data of **4b** we present first indications for a hydridoplumbylene ligand as the missing piece of Group 14 hydridotetrylene coordination chemistry.

An alternative protocol for the synthesis of tungstenocenyl substituted tetrylenes **5a** and **5b** starts with deprotonated tungstenocene dihydride $[Cp_2W(H)Li]_4$ (Scheme 9). In reaction of the anionic hydride with the respective low valent aryltetrylene halides, the tetrylenes of tin and lead were straightforwardly synthesized. Based on NMR spectroscopy the products were formed nearly quantitatively and after crystallization isolated in moderate yield.

To synthesize the homologous tungstenocenyl substituted germylene **5c** the tetrameric anion $[Cp_2W(H)Li]_4$ was reacted with arylgermanium chloride (Scheme 10). After five minutes stirring at rt in the dark green solution, a mixture of products was identified by ^{1}H NMR spectroscopy: two signals exhibiting ^{183}W-satellites were found at −11.03 ppm ($^1J_{W-H}$ = 92 Hz) and +10.02 ppm ($^1J_{W-H}$ = 35 Hz). The signal at low frequency together with the $^1J_{W-H}$ coupling constant is an indicator for a W–H unit and fits in the series of tetrylene tungsten hydride complexes $[Cp_2W(H)$-EAr*]: E = Pb (**5b**) −16.15 ppm, ($^1J_{W-H}$ = 91 Hz), E = Sn (**5a**) −12.37 ppm, ($^1J_{W-H}$ = 90 Hz), E = Ge (**5c**) −11.03 ppm (Table 1). After stirring the product mixture for further 24 h the signal at low frequencies indicating **5c** vanished and only the hydride signal at high frequency remains. Therefore, we suggest germylene **5c** being the kinetically controlled product. Crystallization at −40 °C yields dark green crystals of the arylhydridogermylene complex **9** in moderate yield (53%). The molecular structure of **9** is shown in Fig. 3. Probing the electronic structure of complex **9** DFT calculations together with NBO analysis were performed. Representative NLMOs for the σ- and π-bond were placed in the ESI.† The W=Ge distance of 2.427(3) Å found in **9** can be compared with hydridogermylene coordination at a $CpW(CO)_2$ fragment synthesized by Tobita *et al.* [2.4289(8) Å].[21]

To further investigate the transformation of the kinetically controlled product **5c** *via* a 1,2-H-shift into the thermodynamically controlled product **9**, a solution of a crystalline sample of **9** was treated with light from a mercury-vapor lamp. A mixture between **9** and **5c** (40%/60%) was observed (Scheme 11). Interestingly, from this mixture transformation of **5c** to **9** is much slower (14 d at 40 °C) than in the original reaction mixture (Scheme 10). The faster 1,2-H-shift in the original reaction mixture is probably caused by side products resulting from the synthesis. After addition of AIBN to this mixture (crystalline

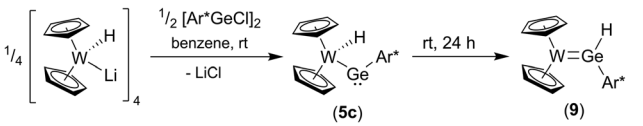

Scheme 10 Reaction of the anion $[Cp_2W(H)Li]_4$ with low valent arylgermanium chloride.

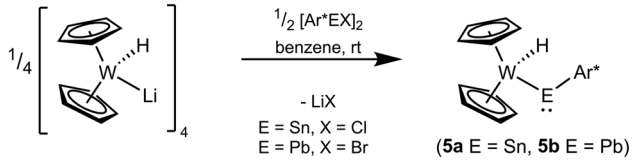

Scheme 9 Synthesis of the tetrylenes of tin **5a** and lead **5b** with $[Cp_2W(H)Li]_4$ as starting material.

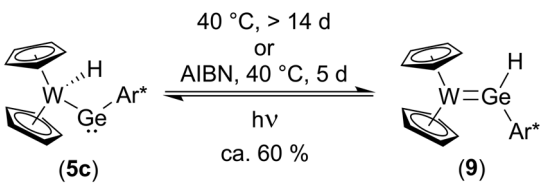

Scheme 11 Reversible 1,2-H-shift.

sample) a much faster conversion of **5c** to **9** was observed making a radical mechanism feasible. With the reversible conversion of **5c** to **9** a rare example for a reversible 1,2-H-shift together with the direct observation of both species, the hydrido-metallogermylene (**5c**) and hydridogermylene (**9**) is presented. DFT calculations confirm both germanium isomers **5c** and **9** being close in energy (see ESI for further details of DFT calculations†). However, in the case of the homologous tin compounds DFT calculations clearly indicate higher stability of the hydrido-metallostannylene isomer (**5a**) compared to a hypothetical arylhydridostannylene-coordination (analogous to Ge-compound **9**). Tilley and co-workers investigated the 1,2-hydrogen migration of heavy group 14 element hydrides coordinated at transition metal centres and have drawn the conclusion, that for tin the hydrido-metallotetrylenes are favoured, in contrast to silicon and germanium, both preferring the hydridotetrylene coordination.[14,19,20,22,84,85] Green *et al.* published a reversible 1,2-H-shift equilibrium between a hydrido-carbene transition metal complex and a methyl ligand.[86] In the case of metallostannylene **5a** our results are in line with the findings made by Tilley *et al.*[84,85] The germanium isomers **9** and **5c** are remarkably close in energy and therefore we were able to characterize both products of 1,2-H shift (Scheme 11).

Protonation of complex **9** was studied in reaction with acid $[H(Et_2O)_2][BAr^F]$ in a mixture of pentane and 1,2-difluorobenzene (Scheme 12). Yellow crystalline material was isolated in moderate yield and based on the NMR data (Table 1) the protonation of the tungsten atom was found. This type of reaction was already presented in the literature in the case of a germylene complex of ruthenium, which was protonated at the transition metal in reaction with a strong Brønsted acid.[14] Cation **4c** is a homologue of the isolated tin cation **4a** and the intermediately formed plumbylene **4b**. The ^{1}H NMR data (signals of GeH and WH, Table 1) of **4c** are in line with the data of the heavier homologues.

Both cations, the low valent lead and tin cation (**1a**, **1b**), were also reacted with zirconocene dihydride $[Cp_2ZrH_2]_2$, but only in the case of the tin salt reaction products could be isolated (Scheme 13).[87–89] Salt **10** was selectively formed no matter which stoichiometry was chosen. After stirring an equimolar mixture of **1a** and dimeric dihydride followed by crystallization from 1,2-diflourobenzene at −40 °C yellow crystals of **10** were isolated in a yield of 69%. The molecular structure in the solid state is depicted in Fig. 4. The dimeric motif of the zirconocene dihydride remains intact. The tin cation coordinates at two Zr–H units forming two hydride bridges showing almost similar Zr–Sn distances [3.0185(2), 3.0325(2) Å]. Due to the hydride bridge

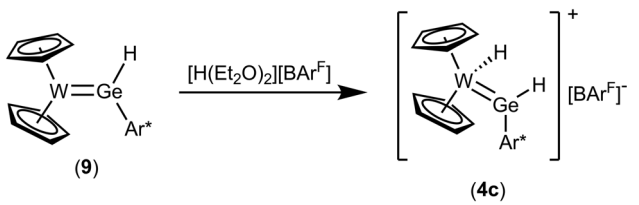

Scheme 12 Protonation of the hydridogermylene complex **9**.

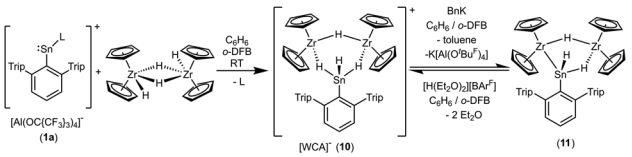

Scheme 13 Synthesis of the hydride bridged trinuclear $SnZr_2$–cation and deprotonation to give **11** ($L = C_6H_6$).

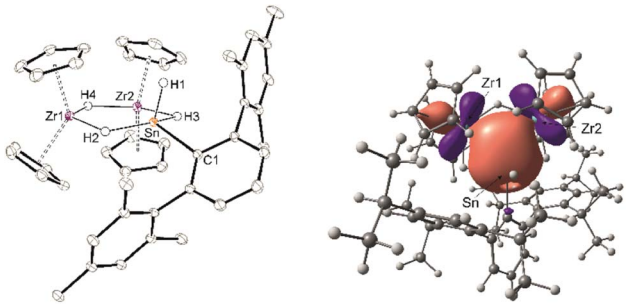

Fig. 4 ORTEP and NLMO exhibiting the three centre two electron bond of cation $[(Cp_2ZrH)_2HSnHAr^*]^+$ of **10**. Thermal ellipsoids are shown at 50% probability level. Hydrogen atoms except the Zr–H and Sn–H units, methyl groups and the anion of **10** have been omitted. Selected interatomic distances [Å] and angles [°]: Zr1–Sn 3.0185(2), Zr2–Sn 3.0325(2), Zr1–Zr2 3.577(2), Zr1–Cp 2.4845(14) – 2.5328(15), Zr2–Cp 2.4760(14) – 2.5162(15), Sn–C1 2.1678(12), Sn–H1 1.57(3), Sn–H2 2.07(3), Sn–H3 1.98(3), Zr1–H2 1.84(3), Zr1–H4 2.00(2), Zr2–H3 1.89(3), Zr2–H4 1.97(2), Zr1–Sn–Zr2 72.5(1), C1–Sn–H1 95.8(10), H2–Sn–H3 144.7(11), H2–Zr1–H4 121.6(11), H3–Zr2–H4 118.3(10).

the Zr–Sn distances are much longer than bond lengths found for typical stannylene coordination [2.794(1)–2.872(1) Å].[30,75,90,91] One hydride ligand is transferred to the tin atom as a terminal coordinating hydride. The hydride atoms inside the six membered ring were found in the final difference Fourier map and the [–Zr–H–Sn–H–Zr–H–] ring shows an almost planar structural motif. This type of dimeric zirconium–hydride complex chelating a main group element fragment was also described by Bulychev *et al.* for $[(Cp_2ZrH)_2H(AlCl_2)]$.[92,93] In the ^{1}H NMR spectrum the Sn–H hydride ligand exhibits a signal at 9.06 ppm ($^1J_{Sn-H}$ = 1344 Hz), which can be compared with values observed for Ar*SnH coordination at group 4 metallocene fragments.[30] The signals for the bridging hydride ligands were observed at lower frequencies Zr–H–Sn (−0.06 ppm) and Zr–H–Zr (−6.24 ppm), lying in the region typical for zirconium hydrides.[92] The ^{119}Sn-NMR signal was observed at relatively low frequency (440 ppm) for low valent tin but can be explained with the high coordination number at the tin atom. The electronic situation was investigated using DFT calculations together with NBO analysis. The lone pair of the tin atom is shared between the two Zr (24, 23%) and the Sn (48%) atoms featuring a three centre two electron bond (see Fig. 4 for NLMO). Both Zr–H units (H2, H3) donate roughly 10% of the two electrons of the bond into the empty p-orbital of tin (see ESI for NLMO†). We interpret compound **10** as a low valent aryl tin hydride Ar*SnH chelated by the cation $[(Cp_2ZrH)_2H]^+$ *via* two hydride bridges.

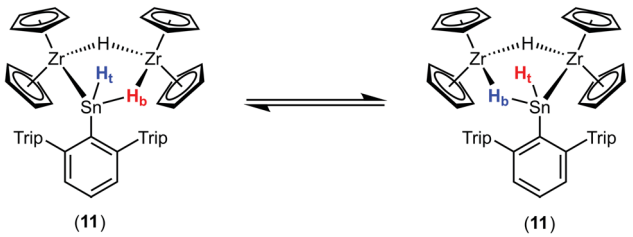

Scheme 14 Dynamic interplay of hydride substituents.

Deprotonation of the cationic hydride **10** was successful with the strong base benzyl potassium to give the trinuclear hydride $[(Cp_2Zr)_2H_2SnHAr^*]$ **11**, which was crystallized from hexane solution at −40 °C (Scheme 13, Fig. 5 and ESI† for molecular structure and NLMOs of **11**). The deprotonation reduced the zirconium atoms to oxidation state III. Reprotonation of **11** was achieved at −40 °C with $[H(Et_2O)_2][BAr^F]$ in 1,2-difluorobenzene as solvent (Scheme 13). Hydride **11** features a Zr–Sn bond of 2.8597(5) Å, which can be compared with stannylene coordination at zirconocene fragments [2.79–2.87 Å].[75,90,91] Complex **11** was also investigated using DFT calculations and NLMOs representing the Zr–Sn σ-bond and the three centre Zr–Sn–Zr two electron bond are presented in ESI.† In the ^{1}H NMR spectrum recorded at rt only broad signals were observed. At −20 °C however for each Cp–ligand and the hydride substituents sharp signals were found [Sn–H: 7.19 ppm $^1J_{Sn-H} \approx 860$ Hz, Zr–H–Zr −12.90 ppm, Zr–H–Sn −3.08 ppm]. *Via* ^{1}H–^{1}H-EXSY-NMR an exchange between the terminal Sn–H and the bridging Zr–H–Sn hydride ligands was detected. The exchange of these hydride ligands (Scheme 14) should be responsible for the broadening of the signals in the rt NMR spectrum.

An alternative synthetic pathway for the formation of complex **11** was found with the reaction of Power's low valent tin hydride **12** with zirconocene dihydride in toluene at room temperature (Scheme 15, ratio Sn/Zr: 1/2).[47] After a spontaneous liberation of dihydrogen, product complex **11** was isolated in high yield (92%) and, based on NMR spectroscopy, in high purity. Crystallization from hexane affords **11** as black/brown crystals. Interestingly, the stepwise formation of **11** was found by stirring a pentane suspension of the zirconium hydride $[Cp_2ZrH_2]_2$ and low valent tin hydride **12** (ratio Sn/Zr: 1/1) at rt for 2 h. Double insertion of the tin moieties into the terminal Zr–H units was found and the

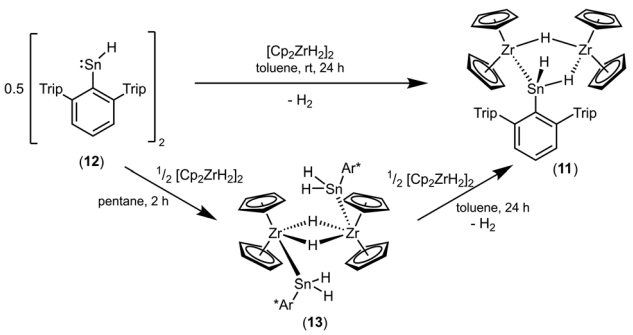

Scheme 15 Alternative route for the synthesis of **11**.

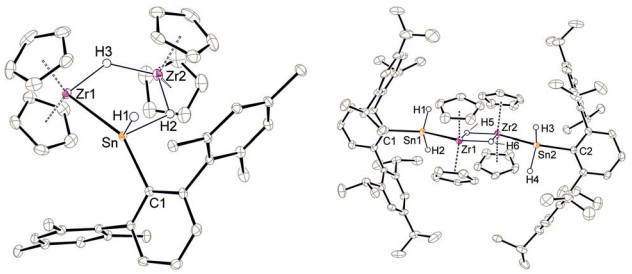

Fig. 5 Molecular structures of **11** and **13**. Thermal ellipsoids are shown at 50% probability level. Hydrogen atoms except the Zr–H and Sn–H units and methyl groups of **11** have been omitted. Selected interatomic distances [Å] and angles [°]: 11, Zr1–Sn 2.8597(5), Zr2–Sn 3.2228(6), Zr1–Cp 2.478(2)–2.551(2), Zr2–Cp 2.494(2)–2.520(2), Sn–C1 2.2257(18), Sn–H1 1.67(3), Sn–H2 2.14(4), Zr1–H3 2.05(3), Zr2–H2 1.77(4), Zr2–H3 1.96(3), Zr1–Sn–C1 152.19(5), Zr1–Sn–H1 109.9(12), Zr1–Sn–H2 99.8(12), H2–Zr2–H3 118.4(16), H3–Zr1–Sn 88.9(9); **13**, Sn1–Zr1 2.9813(4), Sn2–Zr2 2.9794(4), Sn1–C1 2.211(3), Sn2–C2 2.216(3), Zr1–Zr2 3.4468(4), Zr1–Cp 2.480(4)–2.538(4), Zr2–Cp 2.475(4)–2.526(4), Sn1–H1 1.65(4), Sn2–H3 1.66(5), Sn2–H4 1.72(6), Zr1–H5 2.04(4), Zr1–H6 1.97(4), Zr2–H5 1.95(4), Zr2–H6 2.01(4), C1–Sn1–Zr1 139.9(1), C2–Sn2–Zr2 137.8(1).

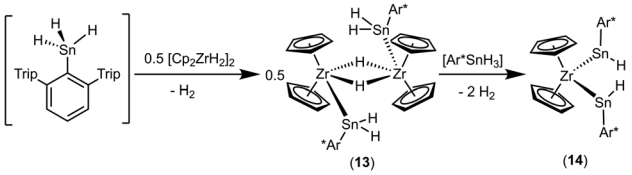

Scheme 16 Reductive elimination hydrogen and formation of the bis(hydridostannylene) complex **14**.

bis(aryldihydridostannyl) complex **13** (Scheme 15, Fig. 5 for molecular structure) was isolated in a yield of 82%. After addition of a further equivalent of zirconocene dihydride to a toluene solution of **13**, liberation of dihydrogen together with formation of **11** was found (Scheme 15).

Complex **13** was also formed in reaction of Ar^*SnH_3 and 0.5 $[Cp_2ZrH_2]_2$. Addition of further equivalents of Ar^*SnH_3 yields together with liberation of hydrogen the hydridostannylene complex $[Cp_2Zr(SnHAr^*)_2]$ (**14**) (Scheme 16).[30] The formation of the Zr–Sn bonds in **13** and **14** is an example for dehydrocoupling reactions between Zr–H and Sn–H species *via* a σ-bond metathesis. This type of M–Sn bond formation was discussed as part of the mechanism in dehydropolymerizations of secondary stannanes catalyzed by zirconocene and hafnocene derivatives.[94–96]

Conclusions

To conclude, hydridotetrylene formation was found reacting the low valent tin cation $[Ar^*Sn]^+$ with tantalocene trihydride, tungstenocene dihydride and the dimeric zirconocene dihydride. In the tantalum and tungsten case, coordination of the low valent hydride [Ar*SnH] at the metal was found and, in the zirconium compound, the tin hydride moiety is chelated by two Zr–H units. The homologous lead cation forms with tungstenocene dihydride an adduct $[Cp_2WH_2PbAr^*]^+$ (**3b**). After

a sequence of deprotonation and reprotonation of this lead adduct, first indications for hydridoplumbylene coordination at a transition metal were observed by low temperature ^{1}H NMR spectroscopy. The cationic hydridostannylene complex of tungstenocenehydride $[Cp_2W(H)Sn(H)Ar^*]^+$ (**4a**) shows reactivity at the tin atom: deprotonation results in formation of the hydrido-tungstenostannylene complex $[Cp_2W(H)SnAr^*]$ (**5a**), hydride addition gives a dihydridostannyl complex and in reaction with styrene hydrostannylation was observed.

Metallotetrylene complexes of tungstenocene $[Cp_2W(H)EAr^*]$ (E = Ge, Sn, Pb) were also synthesized in reaction of the deprotonation product $[Cp_2W(H)Li]_4$ with aryltetrylene halides of germanium, tin, and lead. Only in the case of germanium a reversible transformation of the hydrido-tungstenogermylene $[Cp_2W(H)GeAr^*]$ (**5c**) to the hydridogermylene $[Cp_2W{=}GeHAr^*]$ (**9**) was observed. In comparison to the 1,2-H shift at 40 °C (14 d), after addition of AIBN product formation (40 °C) was completely finished after 5 days. Likely, this 1,2-H shift from the tungsten to the germanium atom is catalyzed by radical species. Under the influence of light, a 1,2-H transfer back to the tungsten atom was found. Therefore, interconversion between metallogermylene (**5c**) and hydridogermylene (**9**) represents a system that exhibits a directly observable and reversible 1,2-H-migration. Corroborated by DFT calculations the 1,2-H shift between **5c** and **9** is almost an isenthalpic reaction.

Dimeric zirconocene dihydride $[Cp_2ZrH_2]_2$ was reacted with the low valent tin cation $[Ar^*Sn]^+$ and the low valent tin hydride $[Ar^*SnH]_2$. Whereas the cationic product was deprotonated to give the dimeric Zr(III) complex $[(\{Cp_2Zr\}_2\{\mu\text{-}H\})(\mu\text{-}H)Sn(H)Ar^*]$ (**11**), this complex together with hydrogen resulted directly from the reaction with $[ArSnH]_2$. Aryltintrihydride Ar^*SnH_3 reacts with dimeric zirconium dihydride to give, as a product of dehydrocoupling reactions *via* σ-bond metathesis, the bis(hydridostannylene) complex of zirconocene $[Cp_2Zr(SnHAr^*)_2]$.

Data availability

Full experimental and computational details are provided as part of the ESI.†

Author contributions

Investigations, writing, original draft preparation, review M. W.; preparation of **1b** S. J.; improved synthesis of **1a** and scientific discussion M. A.; special NMR experiments K. E.; discussion of X-ray measurements H. S.; DFT calculation, manuscript review C. P. S.; supervision, funding acquisition, DFT calculation, manuscript writing and review L. W.

Conflicts of interest

There are no conflicts to declare.

Acknowledgements

M. A. thanks the Fonds der Chemischen Industrie for a scholarship. We acknowledge support of the state of Baden-Württemberg through bwHPC and the German research Foundation (DFG) through grant no INST 40/575-1 FUGG (Justus 2 cluster).

Notes and references

1 M. F. Lappert and P. P. Power, *Dalton Trans.*, 1985, 51–57.
2 W. Petz, *Chem. Rev.*, 1986, **86**, 1019–1047.
3 M. F. Lappert and R. S. Rowe, *Coord. Chem. Rev.*, 1990, **100**, 267–292.
4 J. Baumgartner and C. Marschner, *Rev. Inorg. Chem.*, 2014, **34**, 119.
5 L. Álvarez-Rodríguez, J. A. Cabeza, P. García-Álvarez and D. Polo, *Coord. Chem. Rev.*, 2015, **300**, 1–28.
6 J. A. Cabeza, P. García-Álvarez and D. Polo, *Eur. J. Inorg. Chem.*, 2016, 10–22.
7 B. Blom, M. Stoelzel and M. Driess, *Chem.–Eur. J.*, 2013, **19**, 40–62.
8 J. Y. Corey, *Chem. Rev.*, 2016, **116**, 11291–11435.
9 G. Frenking, R. Tonner, S. Klein, N. Takagi, T. Shimizu, A. Krapp, K. K. Pandey and P. Parameswaran, *Chem. Soc. Rev.*, 2014, **43**, 5106–5139.
10 R. J. Somerville and J. Campos, *Eur. J. Inorg. Chem.*, 2021, **2021**, 3488–3498.
11 M. S. Nechaev, *Organometallics*, 2021, **40**, 3408–3423.
12 A. Doddi, M. Peters and M. Tamm, *Chem. Rev.*, 2019, **119**, 6994–7112.
13 R. S. Simons, J. C. Gallucci, C. A. Tessier and W. J. Youngs, *J. Organomet. Chem.*, 2002, **654**, 224–228.
14 M. E. Fasulo and T. D. Tilley, *Chem. Commun.*, 2012, **48**, 7690–7692.
15 P. B. Glaser and T. D. Tilley, *J. Am. Chem. Soc.*, 2003, **125**, 13640–13641.
16 J. D. Feldman, J. C. Peters and T. D. Tilley, *Organometallics*, 2002, **21**, 4065–4075.
17 T. Watanabe, H. Hashimoto and H. Tobita, *Angew. Chem., Int. Ed.*, 2004, **43**, 218–221.
18 M. Ochiai, H. Hashimoto and H. Tobita, *Angew. Chem., Int. Ed.*, 2007, **46**, 8192–8194.
19 P. G. Hayes, C. W. Gribble, R. Waterman and T. D. Tilley, *J. Am. Chem. Soc.*, 2009, **131**, 4606–4607.
20 P. G. Hayes, R. Waterman, P. B. Glaser and T. D. Tilley, *Organometallics*, 2009, **28**, 5082–5089.
21 H. Hashimoto, T. Tsubota, T. Fukuda and H. Tobita, *Chem. Lett.*, 2009, **38**, 1196–1197.
22 H.-J. Liu, J. Guihaumé, T. Davin, C. Raynaud, O. Eisenstein and T. D. Tilley, *J. Am. Chem. Soc.*, 2014, **136**, 13991–13994.
23 M. C. Lipke, F. Neumeyer and T. D. Tilley, *J. Am. Chem. Soc.*, 2014, **136**, 6092–6102.
24 T. P. Dhungana, H. Hashimoto, M. Ray and H. Tobita, *Organometallics*, 2020, **39**, 4350–4361.
25 P. W. Smith and T. D. Tilley, *J. Am. Chem. Soc.*, 2018, **140**, 3880–3883.
26 B. V. Mork, T. D. Tilley, A. J. Schultz and J. A. Cowan, *J. Am. Chem. Soc.*, 2004, **126**, 10428–10440.
27 P. G. Hayes, C. Beddie, M. B. Hall, R. Waterman and T. D. Tilley, *J. Am. Chem. Soc.*, 2006, **128**, 428–429.

28 R. C. Handford, M. A. Nesbit, P. W. Smith, R. D. Britt and T. D. Tilley, *J. Am. Chem. Soc.*, 2022, **144**, 358–367.
29 Q. Zhu, J. C. Fettinger and P. P. Power, *Dalton Trans.*, 2021, **50**, 12555–12562.
30 J.-J. Maudrich, M. Widemann, F. Diab, R. H. Kern, P. Sirsch, C. P. Sindlinger, H. Schubert and L. Wesemann, *Chem.–Eur. J.*, 2019, **25**, 16081–16087.
31 S. M. I. Al-Rafia, A. C. Malcolm, S. K. Liew, M. J. Ferguson and E. Rivard, *J. Am. Chem. Soc.*, 2011, **133**, 777–779.
32 E. Rivard, *Chem. Soc. Rev.*, 2016, **45**, 989–1003.
33 A. Rit, R. Tirfoin and S. Aldridge, *Angew. Chem., Int. Ed.*, 2016, **55**, 378–382.
34 P. Jutzi, F. Kohl, P. Hofmann, C. Krüger and Y.-H. Tsay, *Chem. Ber.*, 1980, **113**, 757–769.
35 K. Inomata, T. Watanabe, Y. Miyazaki and H. Tobita, *J. Am. Chem. Soc.*, 2015, **137**, 11935–11937.
36 P. Jutzi, R. Dickbreder and H. Nöth, *Chem. Ber.*, 1989, **122**, 865–870.
37 S. Hino, M. Brynda, A. D. Phillips and P. P. Power, *Angew. Chem., Int. Ed.*, 2004, **43**, 2655–2658.
38 C. P. Sindlinger, F. S. W. Aicher and L. Wesemann, *Inorg. Chem.*, 2017, **56**, 548–560.
39 F. Diab, F. S. W. Aicher, C. P. Sindlinger, K. Eichele, H. Schubert and L. Wesemann, *Chem.–Eur. J.*, 2019, **25**, 4426–4434.
40 C. P. Sindlinger, F. S. W. Aicher, H. Schubert and L. Wesemann, *Angew. Chem., Int. Ed.*, 2017, **56**, 2198–2202.
41 J. Li, C. Schenk, F. Winter, H. Scherer, N. Trapp, A. Higelin, S. Keller, R. Pöttgen, I. Krossing and C. Jones, *Angew. Chem., Int. Ed.*, 2012, **51**, 9557–9561.
42 A. Schäfer, W. Saak, D. Haase and T. Müller, *Chem.–Eur. J.*, 2009, **15**, 3945–3950.
43 A. Hinz, *Chem.–Eur. J.*, 2019, **25**, 3267–3271.
44 M. J. Taylor, A. J. Saunders, M. P. Coles and J. R. Fulton, *Organometallics*, 2011, **30**, 1334–1339.
45 H. V. R. Dias and Z. Wang, *J. Am. Chem. Soc.*, 1997, **119**, 4650–4655.
46 R. J. Mangan, A. Rit, C. P. Sindlinger, R. Tirfoin, J. Campos, J. Hicks, K. E. Christensen, H. Niu and S. Aldridge, *Chem.–Eur. J.*, 2020, **26**, 306–315.
47 B. E. Eichler and P. P. Power, *J. Am. Chem. Soc.*, 2000, **122**, 8785–8786.
48 S. Weiß, H. Schubert and L. Wesemann, *Chem. Commun.*, 2019, **55**, 10238–10240.
49 J. Schneider, C. P. Sindlinger, K. Eichele, H. Schubert and L. Wesemann, *J. Am. Chem. Soc.*, 2017, **139**, 6542–6545.
50 I. Krossing, H. Brands, R. Feuerhake and S. Koenig, *J. Fluorine Chem.*, 2001, **112**, 83–90.
51 J. D. Queen, J. C. Fettinger and P. P. Power, *Chem. Commun.*, 2019, **55**, 10285–10287.
52 T. M. Arkhireeva, B. M. Bulychev, A. N. Protsky, G. L. Soloveichik and V. K. Bel'sky, *J. Organomet. Chem.*, 1986, **317**, 33–40.
53 I. Zharov, B. T. King, Z. Havlas, A. Pardi and J. Michl, *J. Am. Chem. Soc.*, 2000, **122**, 10253–10254.
54 T. Müller, in *Advances in Organometallic Chemistry*, ed. R. West, A. F. Hill and F. G. A. Stone, Academic Press, 2005, vol. 53, pp. 155–215.
55 J. B. Lambert and B. Kuhlmann, *Chem. Commun.*, 1992, 931–932, DOI: 10.1039/C39920000931.
56 A. Sekiguchi, T. Fukawa, V. Y. Lee and M. Nakamoto, *J. Am. Chem. Soc.*, 2003, **125**, 9250–9251.
57 A. Schäfer, F. Winter, W. Saak, D. Haase, R. Pöttgen and T. Müller, *Chem.–Eur. J.*, 2011, **17**, 10979–10984.
58 F. Neese, *Wiley Interdiscip. Rev. Comput. Mol. Sci.*, 2018, **8**, e1327.
59 F. Neese, *Wiley Interdiscip. Rev. Comput. Mol. Sci.*, 2012, **2**, 73–78.
60 ADF2019.3, Vrije Universiteit Amsterdam, 2019, http://www.scm.com.
61 L. Rocchigiani, W. T. Klooster, S. J. Coles, D. L. Hughes, P. Hrobárik and M. Bochmann, *Chem.–Eur. J.*, 2020, **26**, 8267–8280.
62 M. Widemann, K. Eichele, H. Schubert, C. P. Sindlinger, S. Klenner, R. Pöttgen and L. Wesemann, *Angew. Chem., Int. Ed.*, 2021, **60**, 5882–5889.
63 J. Mason, *Multinuclear NMR*, Plenum Press, New York, NY 1987.
64 R. K. Harris and B. E. Mann, *NMR and the periodic table*, Academic Press, London, 1978.
65 T. A. Mobley, R. Gandour, E. P. Gillis, K. Nti-Addae, R. Palchaudhuri, P. Rajbhandari, N. Tomson, A. Vargas and Q. Zheng, *Organometallics*, 2005, **24**, 3897–3906.
66 M. P. Johnson and D. F. Shriver, *J. Am. Chem. Soc.*, 1966, **88**, 301–304.
67 M. S. Holt, W. L. Wilson and J. H. Nelson, *Chem. Rev.*, 1989, **89**, 11–49.
68 M. L. McCrea-Hendrick, C. A. Caputo, J. Linnera, P. Vasko, C. M. Weinstein, J. C. Fettinger, H. M. Tuononen and P. P. Power, *Organometallics*, 2016, **35**, 2759–2767.
69 S. M. Mansell, R. H. Herber, I. Nowik, D. H. Ross, C. A. Russell and D. F. Wass, *Inorg. Chem.*, 2011, **50**, 2252–2263.
70 A. Y. Khalimon, K. Y. Dorogov, A. V. Churakov, L. G. Kuzmina, D. A. Lemenovskii, J. A. K. Howard and G. I. Nikonov, *Dalton Trans.*, 2007, 2440–2449.
71 P. Kircher, G. Huttner, B. Schiemenz, K. Heinze, L. Zsolnai, O. Walter, A. Jacobi and A. Driess, *Chem. Ber.*, 1997, **130**, 687–699.
72 A. C. Filippou, P. Portius, A. I. Philippopoulos and H. Rohde, *Angew. Chem., Int. Ed.*, 2003, **42**, 445–447.
73 A. C. Filippou, A. I. Philippopoulos and G. Schnakenburg, *Organometallics*, 2003, **22**, 3339–3341.
74 E. D. Glendening, J. K. Badenhoop, A. E. Reed, J. E. Carpenter, J. A. Bohmann, C. M. Morales, P. Karafiloglou, C. R. Landis and F. Weinhold, NBO 7.0, 2018.
75 H. Arp, J. Baumgartner, C. Marschner, P. Zark and T. Müller, *J. Am. Chem. Soc.*, 2012, **134**, 10864–10875.
76 B. E. Eichler, A. D. Phillips, S. T. Haubrich, B. V. Mork and P. P. Power, *Organometallics*, 2002, **21**, 5622–5627.
77 Y. N. Lebedev, U. Das, G. Schnakenburg and A. C. Filippou, *Organometallics*, 2017, **36**, 1530–1540.
78 M. Brookhart, B. Grant and A. F. Volpe, *Organometallics*, 1992, **11**, 3920–3922.

79 T. Fukuda, H. Hashimoto and H. Tobita, *J. Organomet. Chem.*, 2017, **848**, 89–94.
80 T. Fukuda, T. Yoshimoto, H. Hashimoto and H. Tobita, *Organometallics*, 2016, **35**, 921–924.
81 S. Wang, M. L. McCrea-Hendrick, C. M. Weinstein, C. A. Caputo, E. Hoppe, J. C. Fettinger, M. M. Olmstead and P. P. Power, *J. Am. Chem. Soc.*, 2017, **139**, 6586–6595.
82 L. Pu, P. P. Power, I. Boltes and R. Herbst-Irmer, *Organometallics*, 2000, **19**, 352–356.
83 J. Vícha, J. Novotný, S. Komorovsky, M. Straka, M. Kaupp and R. Marek, *Chem. Rev.*, 2020, **120**, 7065–7103.
84 H.-J. Liu, C. Landis, C. Raynaud, O. Eisenstein and T. D. Tilley, *J. Am. Chem. Soc.*, 2015, **137**, 9186–9194.
85 P. W. Smith, R. C. Handford and T. D. Tilley, *Organometallics*, 2019, **38**, 4060–4065.
86 N. J. Cooper and M. L. H. Green, *Dalton Trans.*, 1979, 1121–1127.
87 D. G. Bickley, N. Hao, P. Bougeard, B. G. Sayer, R. C. Burns and M. J. McGlinchey, *J. Organomet. Chem.*, 1983, **246**, 257–268.
88 S. B. Jones and J. L. Petersen, *Inorg. Chem.*, 1981, **20**, 2889–2894.
89 B. D. James, R. K. Nanda and M. G. H. Walbridge, *Inorg. Chem.*, 1967, **6**, 1979–1983.
90 R. M. Whittal, G. Ferguson, J. F. Gallagher and W. E. Piers, *J. Am. Chem. Soc.*, 1991, **113**, 9867–9868.
91 J. Bareš, P. Richard, P. Meunier, N. Pirio, Z. Padělková, Z. Černošek, I. Císařová and A. Růžička, *Organometallics*, 2009, **28**, 3105–3108.
92 A. I. Sizov, T. M. Zvukova, A. V. Khvostov, V. K. Belsky, A. I. Stash and B. M. Bulychev, *J. Organomet. Chem.*, 2003, **681**, 167–173.
93 A. I. Sizov, T. M. Zvukova, V. K. Belsky and B. M. Bulychev, *J. Organomet. Chem.*, 2001, **619**, 36–42.
94 T. Imori, V. Lu, H. Cai and T. D. Tilley, *J. Am. Chem. Soc.*, 1995, **117**, 9931–9940.
95 T. Imori and T. D. Tilley, *Chem. Commun.*, 1993, 1607–1609.
96 J. Guihaumé, C. Raynaud, O. Eisenstein, L. Perrin, L. Maron and T. D. Tilley, *Angew. Chem., Int. Ed.*, 2010, **49**, 1816–1819.